ANL/NSE-20/5

SAM Code Validation on Frictional Pressure Drop through Pebble Beds

Nuclear Science and Engineering Division

About Argonne National Laboratory
Argonne is a U.S. Department of Energy laboratory managed by UChicago Argonne, LLC under contract DE-AC02-06CH11357. The Laboratory's main facility is outside Chicago, at 9700 South Cass Avenue, Argonne, Illinois 60439. For information about Argonne and its pioneering science and technology programs, see www.anl.gov.

ANL-NSE-20/5

SAM Code Validation on Frictional Pressure Drop through Pebble Beds

prepared by
Ling Zou and Rui Hu
Nuclear Science and Engineering Division, Argonne National Laboratory

March 2020

EXECUTIVE SUMMARY

The System Analysis Module (SAM) is currently under development at Argonne National Laboratory as a modern system-level modeling and simulation tool for safety analyses of advanced non-light water reactors. This report presents a recent effort to validate the capability of SAM to predict the frictional pressure drop through pebble beds. Selected experimental data were used for code validation, including data from test facilities at Texas A&M University, Missouri University of Science and Technology, and North-West University of South Africa. SAM implements three empirical correlations to predict frictional pressure drop: the classical Ergun correlation; the KTA correlation, which is widely used in high-temperature gas-cooled reactor applications; and the Eisfeld and Schnitzlein correlation, which explicitly considers wall effect. Code validation was performed using all three correlations. For all selected experimental data, the KTA correlation shows the best performance and agrees very well with experimental measurement; the Eisfeld and Schnitzlein correlation, explicitly considering wall effects, shows acceptable accuracy, while there is no evidence that it is better than the KTA correlation; the Ergun correlation, however, over-predicts frictional pressure drop for most selected data points.

CONTENTS

FIGURES

TABLES

1 Introduction

In the United States in recent years, there has been increased interest in the research and development of advanced non-light water reactor (non-LWR) technologies. Among these advanced non-LWR concepts, only recently has the pebble-bed high-temperature reactor seen significant advances, including the Kairos Power fluoride-salt-cooled high-temperature reactor (KP-FHR) and X-energy's Xe-100 high-temperature gas-cooled reactor (HTGR) designs. From a thermal-hydraulics analysis perspective, a pebble-bed reactor core design generally experiences more significant multidimensional effects than LWR design. The pebble-bed core is typically modeled by using the porous medium approach for both designs (e.g., Gao and Shi [1]) and accident analysis (e.g., Zheng, Shi, and Dong [2]) for multidimensional effects.

The System Analysis Module (SAM), a modern system analysis code being developed at Argonne National Laboratory for advanced non-LWR safety analysis [3], has also drawn interest from U.S. Nuclear Regulatory Commission (U.S. NRC) as a potential licensing tool for advanced non-LWR designs [4]. The code is still under active development to support applications of the pebble-bed reactor analysis. Previous efforts have included introducing the porous-medium-based model into SAM code, validating the effective thermal conductivity of pebble beds [5], and incorporating frictional pressure drop correlations into the code.

The main objective of the current work is to validate the computer code for predicting the frictional pressure drop across pebble beds by using existing experimental data on pebble-bed reactor designs. Pressure drop across a pebble-bed core is one of the most important design parameters because it is closely related to the flow distribution, pumping power, and operational cost of the reactor [6]. In the field of chemical engineering, the pressure drop through packed beds has been the subject of many theoretical analysis and experimental investigations. In the field of nuclear engineering, there has also been dedicated work on this topic to provide empirical correlations or experimental data for code validation.

This report is structured as follows: Section 2 introduces the porous medium-based physics model; Section 3 provides a general review on empirical correlations for predicting frictional pressure drop through pebble beds and selected correlations currently implemented in SAM; Section 4 provides validation results comparing SAM results with selected experimental data; and Section 5 provides summarizes this work. For further reference, supplemental data, results, and plots are provided in Appendices A, B, and C.

2 Physics Model

In nuclear reactor thermal-hydraulics analysis, it is a common approach to using porous-medium flow to model the fluid flow and heat transfer in very complex but regular pattern geometries, such as the pebble-bed core in HTGRs and tube bundles in steam generators. In SAM, a porous-medium-flow model has been recently implemented to support the modeling and simulation needs for the pebble-bed reactors [5], based on an existing three-dimensional (3D) flow model previously implemented in SAM [7].

For completeness, the porous-medium-flow model is given. The following equations describe the mass, momentum, and energy balance of the fluid phase:

$$\epsilon \frac{\partial \rho}{\partial t} + \nabla \cdot (\rho \vec{u}) = 0 \tag{1}$$

$$\rho \frac{\partial \vec{u}}{\partial t} + \frac{\rho}{\epsilon}(\vec{u} \cdot \nabla)\vec{u} + \epsilon \nabla p - \epsilon \rho \vec{g} + \beta \vec{u} + \alpha |\vec{u}| \vec{u} = 0 \tag{2}$$

$$\epsilon \rho c_p \frac{\partial T}{\partial t} + \rho c_p \vec{u} \cdot \nabla T - \nabla \cdot (\epsilon k \nabla T) - q''' + a_w h (T - T_s) = 0 \,. \tag{3}$$

When needed, an addition solid energy equation is added to consider heat conduction within solid structure and its convective heat transfer with the fluid phase:

$$(1 - \epsilon)\rho_s c_{p,s} \frac{\partial T_s}{\partial t} - \nabla \cdot \left(k_{eff} \nabla T_s\right) + a_w h (T_s - T) - q_s''' = 0 \,, \tag{4}$$

where

ϵ is the porosity of the pebble bed,

$\vec{u}$ is the so-called superficial velocity, which is related to the intrinsic velocity, $\vec{U}$, as $\vec{u} = \vec{U}\epsilon$.

The last two terms in the momentum equation (2) represent the linear (Darcy) and nonlinear (Forchheimer) drag terms, respectively. Currently, several empirical correlations have been implemented in SAM for the two coefficients, α and β, and these correlations are the main focus in this validation study. The heat transfer between the fluid and solid phase is represented by the $a_w h(T - T_s)$ term in the fluid energy equation, (3), as well as the $a_w h(T_s - T)$ term in the solid energy equation, (4), in which a_w is heat transfer area per unit volume.

The solid energy equation is not included in the remainder of this report as it is irrelevant to this validation study. The fluid energy equation, however, is included, although all validation tests are conducted in isothermal conditions.

3 Correlations for Predicting Frictional Pressure Drop

It was Blake [8] who first successfully treated the pressure drop problem in porous beds (or "packing materials," as he referred to them). Blake suggested a pair of two non-dimensional parameters [8, 9, 10]:

$$f_k \equiv \frac{\Delta p}{\rho u^2} \frac{d_p}{L} \frac{\epsilon^3}{1 - \epsilon} \tag{5}$$

and

$$\mathrm{Re}_m \equiv \frac{\rho u d_p}{\mu (1 - \epsilon)} \,, \tag{6}$$

and proposed that f_k could be correlated as a function of Re_m, that is, $f_k = f(\mathrm{Re}_m)$. The term f_k was referred to as the Blake-type friction factor by Ergun, and Re_m has been referred to as the modified Reynolds number by many authors. Most empirical correlations proposed to predict frictional pressure drop through pebble beds have followed such a formula.

There are also different ways to define the non-dimensional parameters. Two additional such parameters are introduced here as they are closely related to the validation study

presented in this report. In some studies, for example, the KTA correlation [10, 11], the non-dimensional pressure drag coefficient is given as

$$\Psi \equiv \frac{\Delta p}{\frac{1}{2}\rho u^2}\frac{d_p}{L}\frac{\epsilon^3}{1-\epsilon}, \tag{7}$$

and it is obvious that,

$$\Psi = 2f_k \quad \text{or} \quad f_k = \Psi/2 . \tag{8}$$

In some other studies, for example, Kang [15] and Hassan and Kang [6], the modified friction factor is used:

$$f_m \equiv \frac{\Delta p}{L}\frac{d_p^2}{\mu u}\frac{\epsilon^3}{(1-\epsilon)^2} . \tag{9}$$

It is also clear that

$$f_m = f_k \mathrm{Re}_m . \tag{10}$$

Currently within SAM, we have selected and implemented three empirical correlations to predict frictional pressure drop through porous pebble beds: (1) the classical Ergun correlation; (2) the KTA correlation, which is widely used in pebble-bed reactor analysis applications; and (3) the Eisfeld and Schnitzlein correlation, which explicitly considers the wall effect on pressure drop in pebble beds. We do not intend to collect and implement all possible such pressure drop correlations in SAM, nor do we intend to validate all such correlations. The main purpose is to validate the correctness of computer code implementation by comparing these three correlations with available experimental data.

3.1 Ergun Correlation

The Ergun correlation represents a classical correlation for predicting frictional pressure drop across packed pebble beds. It was developed based on 640 experimental data points on various-sized spheres, sand, pulverized coke, and various gases (carbon dioxide, nitrogen, methane, and hydrogen), and considered pressure drop through porous packed beds as a result of simultaneous kinetic and viscous energy losses [9]:

$$\frac{\Delta p}{L} = 150\frac{(1-\epsilon)^2}{\epsilon^3}\frac{\mu}{d_p^2}u + 1.75\frac{1-\epsilon}{\epsilon^3}\frac{\rho}{d_p}u^2 . \tag{11}$$

Based on Equation (11), the linear viscous drag coefficient and quadratic drag coefficient of the Ergun correlation are

$$\beta = 150\frac{(1-\epsilon)^2}{\epsilon^2}\frac{\mu}{d_p^2} \tag{12}$$

and

$$\alpha = 1.75\frac{1-\epsilon}{\epsilon^2}\frac{\rho}{d_p}, \tag{13}$$

respectively. The non-dimensional frictional pressure drop coefficient is therefore

$$\Psi = \frac{300}{\mathrm{Re}_m} + 3.5\,, \tag{14}$$

and the modified friction factor is

$$f_m = \frac{\Psi}{2}\mathrm{Re}_m = 150 + 1.75\mathrm{Re}_m\,. \tag{15}$$

Validity Region

Reynolds number: not provided[1]

Porosity of the bed: not provided

Uncertainty range: not provided.

3.2 KTA Correlation

The KTA correlation has been developed based on the review of published data and correlations from about 30 papers [10]. The KTA correlation is given as [10, 11].

$$\frac{\Delta p}{L} = \Psi \frac{1-\epsilon}{\epsilon^3}\frac{1}{d_p}\frac{\rho u^2}{2}\,, \tag{16}$$

with the non-dimensional drag coefficient,

$$\Psi = \frac{320}{\mathrm{Re}_m} + \frac{6}{\mathrm{Re}_m^{0.1}}\,. \tag{17}$$

Although the expression does not explicitly include the wall effect, the discussion provided in Fenech [10] suggests that the wall effect has been implicitly considered in the average void fraction of the pebble bed, which is dependent on the pebble diameter-to-bed diameter ratio.

The linear viscous drag coefficient and quadratic drag coefficient are

$$\beta = 160\frac{(1-\epsilon)^2}{\epsilon^2}\frac{\mu}{d_p^2} \tag{18}$$

and

$$\alpha = \frac{3}{\mathrm{Re}_m^{0.1}}\frac{1-\epsilon}{\epsilon^2}\frac{\rho}{d_p}\,, \tag{19}$$

respectively. The modified friction factor is given as

$$f_m = \frac{\Psi}{2}\mathrm{Re}_m = 160 + 3\mathrm{Re}_m^{0.9}\,. \tag{20}$$

Validity Region

Reynolds number: $1 < \mathrm{Re}_m < 10^5$

[1] From the plots of the original paper by Ergun, it seems that the correlation was fitted from data in the range of $1 < \mathrm{Re}_m < 2500$.

Porosity of the bed: $0.36 < \epsilon < 0.42$
Diameter ratio: curving fitting, see [11]
Height of bed: H > $5d_p$
Uncertainty range:
$\pm 15\%$ with a confidence level of 95%.

3.3 Eisfeld and Schnitzlein Correlation

Eisfeld and Schnitzlein [12] performed a detailed analysis of more than 2,300 experimental data points and found that the influence of the container walls on the pressure drop of packed beds should be considered. Their investigation showed that Reichelt's approach to correcting the original Ergun equation for the wall effect is most promising, and they provided improved correlations obtained by fitting the coefficients to their database.

Eisfeld and Schnitzlein provided three fitted correlations, one for spherical particles, one for cylinder particles, and one for both spherical and cylinder particles. As our main objective is to provide modeling and simulation capability for the (spherical) pebble-bed reactor designs, we include only the correlation for spherical particles. The Eisfeld and Schnitzlein correlation for spherical particles is given as

$$\frac{\Delta p}{L} = \left[\frac{154A_w^2}{\mathrm{Re}_m} + \frac{A_w}{B_w}\right]\frac{1-\epsilon}{\epsilon^3}\frac{\rho u^2}{d_p} \tag{21}$$

with

$$A_w = 1 + \frac{2\left(d_p/D_{bed}\right)}{3(1-\epsilon)} \tag{22}$$

$$B_w = \left[1.15\left(\frac{d_p}{D_{bed}}\right)^2 + 0.87\right]^2 . \tag{23}$$

Thus, the linear viscous drag coefficient and quadratic drag coefficient are

$$\beta = 154A_w^2\frac{(1-\epsilon)^2}{\epsilon^2}\frac{\mu}{d_p^2} \tag{24}$$

and

$$\alpha = \frac{A_w}{B_w}\frac{1-\epsilon}{\epsilon^2}\frac{\rho}{d_p}, \tag{25}$$

respectively. The non-dimensional frictional pressure drop coefficient is therefore

$$\Psi = \frac{308A_w^2}{\mathrm{Re}_m} + \frac{2A_w}{B_w}, \tag{26}$$

and the modified friction factor is

$$f_m = \frac{\Psi}{2}\mathrm{Re}_m = 154A_w^2 + \frac{A_w}{B_w}\mathrm{Re}_m\,. \tag{27}$$

Validity Region

Reynolds number: $0.01 < \mathrm{Re}_{dp} < 17635$ in which $\mathrm{Re}_{dp} = \rho u d_p/\mu$

Porosity of the bed: $0.330 < \epsilon < 0.882$

Diameter ratio: $1.624 \leq D_{bed}/d_p \leq 250$

Height of bed: not provided

Uncertainty Range

Relative root mean square deviation, $\sigma = 0.1613$

Maximum relative deviation at 95% confidence, $f_{95} = 0.31$

Maximum relative deviation at 99% confidence, $f_{99} = 0.48$

4 Code Validation

As discussed in Section 1, abundant experimental data are available for frictional-pressure-drop code validation purposes. As a matter of fact, most existing empirical correlations for predicting frictional pressure drop through pebble beds have indeed been developed based on hundreds or thousands of data points. For the limited work scope of this validation effort, we did not intend to provide a survey of existing data or to include all of them for validation. We limited this code validation effort to data that are complete, of high quality, and available. For this study, we chose experimental data obtained from test facilities at Texas A&M University (TAMU), which use both water and air as working fluid, and experimental data obtained from a test facility at Missouri University of Science and Technology (Missouri S&T), which uses air as working fluid, as well as experimental data obtained from the HPTU facility of North-West University of South Africa.

4.1 TAMU Water/Air Experiments

A pressure drop test facility was designed and constructed at TAMU to study single-phase-flow frictional pressure drop in a packed bed. The test section is a cylindrical column made of polymethyl methacrylate (PMMA) and randomly packed with spherical PMMA beads [6]. The cylinder test section is 12.065 cm in diameter and 152.4 cm in height. The spherical PMMA beads diameters are 0.635, 1.27, 1.905, and 3.302 cm for four separate tests. The test facility is flexible such that both water and air can be used as the working fluid. Experimental data from Kang [15] also suggest that the test section could be either horizontally or vertically oriented. To accurately measure the bed porosity, three methods were used: the water displacement method, the weighting method, and the particle counting method. The dimensions of the test section are summarized in Table 1see also Figure 1.

Table 1 Dimensions of test section of TAMU water/air pressure drop experiment

Bed height, L (cm)	Bed diameter, D (cm)	Particle diameter, d_p (cm)	D/d_p [-]	Bed porosity [-]
152.4	12.065	0.635	19	0.385
		1.27	9.5	0.397
		1.905	6.33	0.416
		3.302	3.65	0.465

Experiments were carried out using both water and air as the working fluid under different inlet velocities conditions. Fluid temperature varies from test to test in the range of 20-40 °C. System pressure was not explicitly given; however, from what is provided for fluid properties in Kang [15], it is reasonable to assume the system pressure is at atmospheric pressure, 10^5 Pa. The test conditions for all available TAMU pressure drop tests are given in Appendix A, while more details are available in Kang [15].

Because of the large number of available test data, we did not intend to perform case-by-case validations. Instead, inlet fluid temperatures (T_{inlet}) were given as a fixed value at 30°C, while inlet superficial velocities (u_{inlet}) were chosen to cover the modified Reynolds number ranges investigated in experimental tests. The outlet pressure (p_{outlet}) is set as a fixed value at 10^5 Pa. These selected simulation conditions are listed in Table 2 for water tests and Table 3 for air tests. Because of the very simple geometry (a cylindrical column) of the test bed, all SAM simulations were performed using 2D-RZ geometry, as shown in Figure 1, with uniformly distributed QUAD mesh, 8(R) × 60(Z), and horizontally oriented. It is also worth noting that, in all simulations, non-uniform bed porosity was not considered, and slip wall boundary conditions are applied for the momentum equations on the wall. The same conditions (uniform bed porosity and slip wall boundary conditions) have been applied to all SAM simulations, including the Missouri S&T and North-West University validation tests in following sections. Simulations were also performed for selected cases to consider 3D effects and vertically oriented conditions, and it was confirmed that the simulation results on frictional drop were the same (within numerical error tolerance). For each selected simulation condition, SAM simulations were performed using all three correlations, that is, the KTA, Ergun, and Eisfeld and Schnitzlein correlations.

Table 2 Selected conditions for SAM simulations on TAMU water test cases

d_p = 6.35 mm, D/d_p = 19		d_p = 12.7 mm, D/d_p = 9.5		d_p = 19.05 mm, D/d_p = 6.33		d_p = 33.02 mm, D/d_p = 3.65	
Inlet superficial velocity (m/s)	Re_m	Inlet superficial velocity (m/s)	Re_m	Inlet superficial velocity (m/s)	Re_m	Inlet superficial velocity (m/s)	Re_m
0.05	6.4465E+02	0.1	2.6299E+03	0.1	4.0732E+03	0.1	7.7069E+03
0.1	1.2893E+03	0.2	5.2599E+03	0.2	8.1465E+03	0.2	1.5414E+04
0.2	2.5786E+03	0.3	7.8898E+03	0.3	1.2220E+04	0.3	2.3121E+04
0.25	3.2233E+03	0.4	1.0520E+04	0.4	1.6293E+04	0.4	3.0828E+04

Table 3 Selected conditions for SAM simulations on TAMU air test cases

d_p = 6.35 mm D/d_p = 19		d_p = 12.7 mm D/d_p = 9.5		d_p = 19.05 mm D/d_p = 6.33	
Inlet superficial velocity (m/s)	Re_m	Inlet superficial velocity (m/s)	Re_m	Inlet superficial velocity (m/s)	Re_m
0.4	2.6387E+02	0.4	5.3823E+02	0.4	8.3362E+02
0.6	3.9580E+02	0.8	1.0765E+03	0.8	1.6672E+03
0.8	5.2773E+02	1.2	1.6147E+03	1.2	2.5008E+03
1.0	6.5966E+02	1.6	2.1529E+03	1.6	3.3345E+03
1.2	7.9160E+02	2.0	2.6912E+03	2.0	4.1681E+03
		2.4	3.2294E+03	2.4	5.0017E+03
		2.8	3.7676E+03	2.8	5.8353E+03
		3.2	4.3059E+03	3.2	6.6689E+03
		3.6	4.8441E+03	3.6	7.5025E+03
		4.0	5.3823E+03	4.0	8.3362E+03

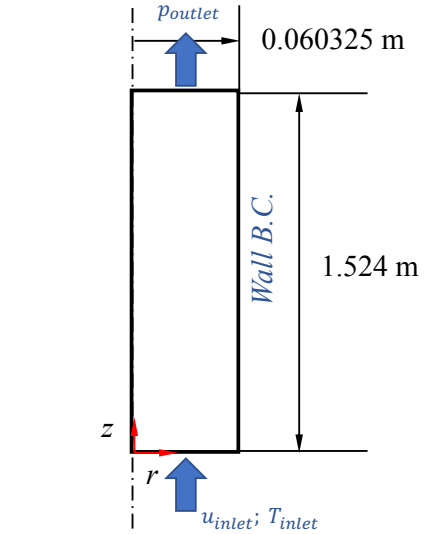

Figure 1 Dimensions and boundary conditions setup for TAMU pressure drop tests

The comparison of SAM-predicted modified friction factors between the three correlations and experimental measurements is plotted in Figure 2for water cases and in Figure 5for air cases, respectively. For further reference, for each of these figures, zoom-in views for modified Reynolds numbers between 0 and 5,000 for water and between 0 and 2,000 for air are also given in Appendix A. TAMU experimental data and SAM results are also provided as tables in Appendix A. Before discussing validation results, SAM-predicted modified friction factors are compared with numbers computed from analytical expression, and they are fairly identical to the fifth significant figures (expect for several data points, for which the difference is still very small).

4.1.1 Validation of Water Experiments

We first observed that water test cases with D/d_p = 3.65 show completely different trends from other data, and none of the tested correlations was able to capture such a deviation, which might be due to the very small D/d_p ratio used in the experiments; this set of data is excluded in the following discussions if not explicitly stated.

- Figure 2 (and Figure A-1) shows SAM results using the KTA correlation, which exhibits very good agreement with the remaining experimental data except for cases with D/d_p = 3.65. Most of the remaining data is within the ±15% uncertainty range of the KTA correlation.
- The Ergun correlation, as shown in Figure 3 (and Figure A-2), however, greatly overestimates the frictional pressure drop except for small modified Reynolds numbers. The errors are as large as 40% for larger modified Reynolds numbers.
- Figure 4 (and Figure A-3) shows the comparison between the Eisfeld and Schnitzlein correlation results and experimental data, which, overall, shows acceptable accuracy. For the small modified Reynolds number range ($0 < Re_m < \sim 1500$), it slightly underestimates the friction factor, while in the mid-modified Reynolds number range ($\sim 1500 < Re_m < \sim 5000$), it overlays with experimental measurements fairly well within its uncertainty range (±16.13%). However, for larger modified Reynolds numbers, it starts to deviate from experimental measurements and barely overlays with them.

4.1.2 Validation of Air Experiments

Validation of the air test cases is quite similar to that of the water test cases. Also, the air test data show larger scattering compared to water test data.

- Figure 5 (and Figure A-4) shows that the KTA correlation is able to predict the friction factor, within its uncertainty range, over the entire modified Reynolds number domain investigated for the air test cases.
- Figure 6 (and Figure A-5) shows that the Ergun correlation can produce good accuracy only for small modified Reynolds numbers; it greatly overestimates the friction factor for larger modified Reynolds numbers.
- Figure 7 (and Figure A-6) shows that the Eisfeld and Schnitzlein correlation produces better accuracy for small modified Reynolds numbers, and starts to deviate from experimental measurements for larger modified Reynolds numbers.

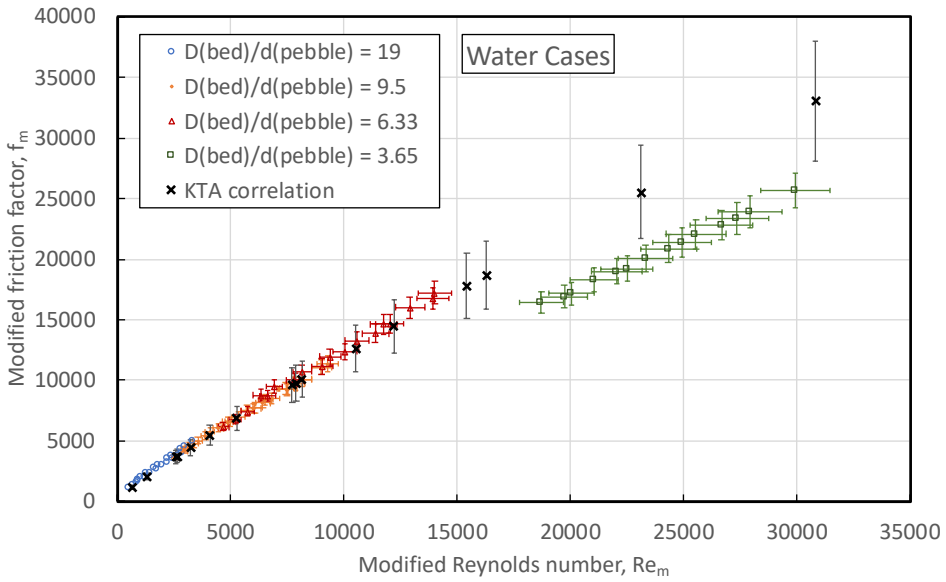

Figure 2 Comparison of SAM-predicted modified friction factor (f_m) between the KTA correlation and TAMU water experimental measurements. A ±15% uncertainty bar is added for SAM-predicted results using the KTA correlation. Uncertainties for experimental data are ±5.1% for Re_m and ±5.5% for f_m, as reported in Hassan and Kang [6].

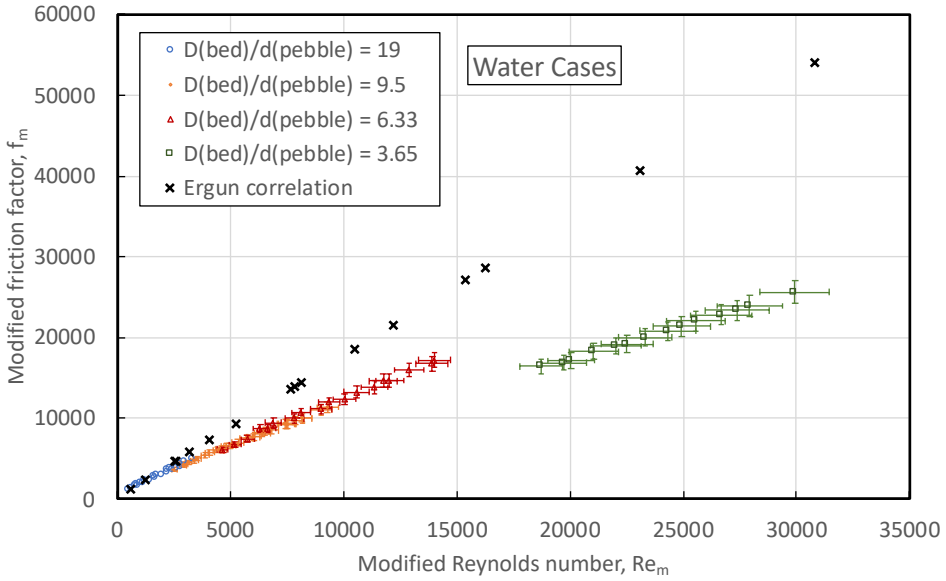

Figure 3 Comparison of SAM-predicted modified friction factor (f_m) between the Ergun correlation and TAMU water experimental measurements. Uncertainty of the Ergun correlation is not available and therefore not plotted. Uncertainties for experimental data are ±5.1% for Re_m and ±5.5% for f_m, as reported in Hassan and Kang [6].

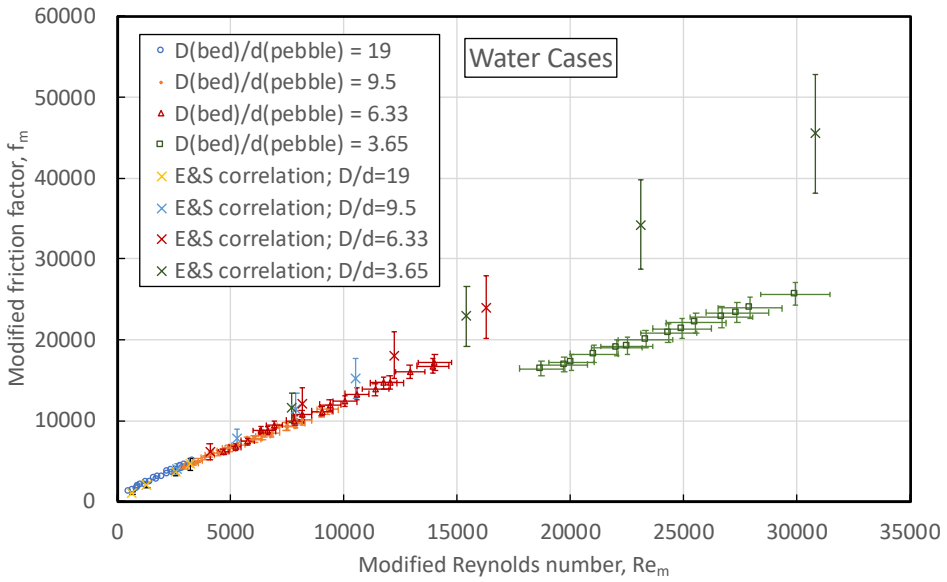

Figure 4 Comparison of SAM-predicted modified friction factor (f_m) between the Ergun correlation and TAMU water experimental measurements. A ±16.13% uncertainty bar is added for SAM-predicted results using the Eisfeld and Schnitzlein correlation. Uncertainties for experimental data are ±5.1% for Re_m and ±5.5% for f_m, as reported in Hassan and Kang [6].

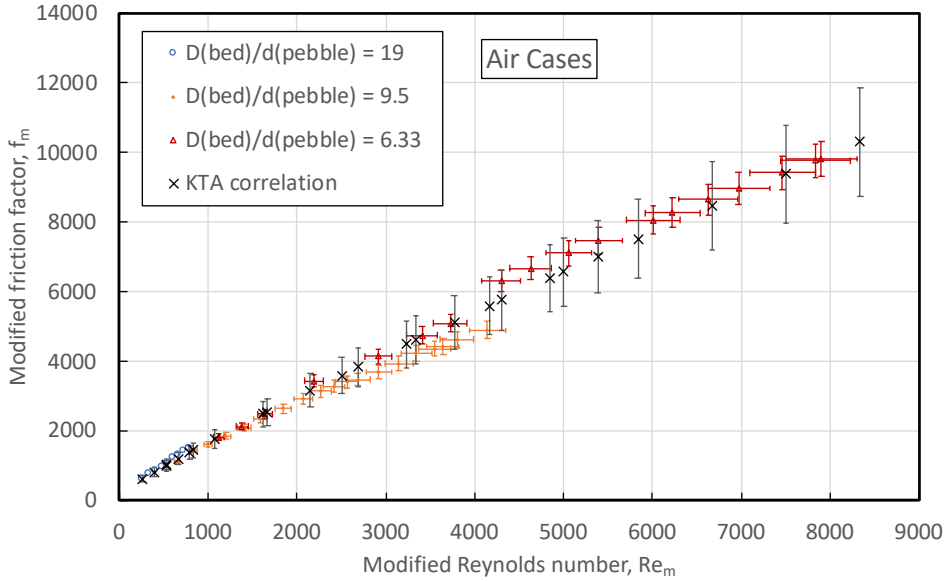

Figure 5 Comparison of SAM-predicted modified friction factor (f_m) between the KTA correlation and TAMU air experimental measurements. A ±15% uncertainty bar is added for SAM-predicted results using the KTA correlation. Uncertainties for experimental data are ±5.0% for Re_m, and ±5.1% for f_m, as reported in Hassan and Kang [6].

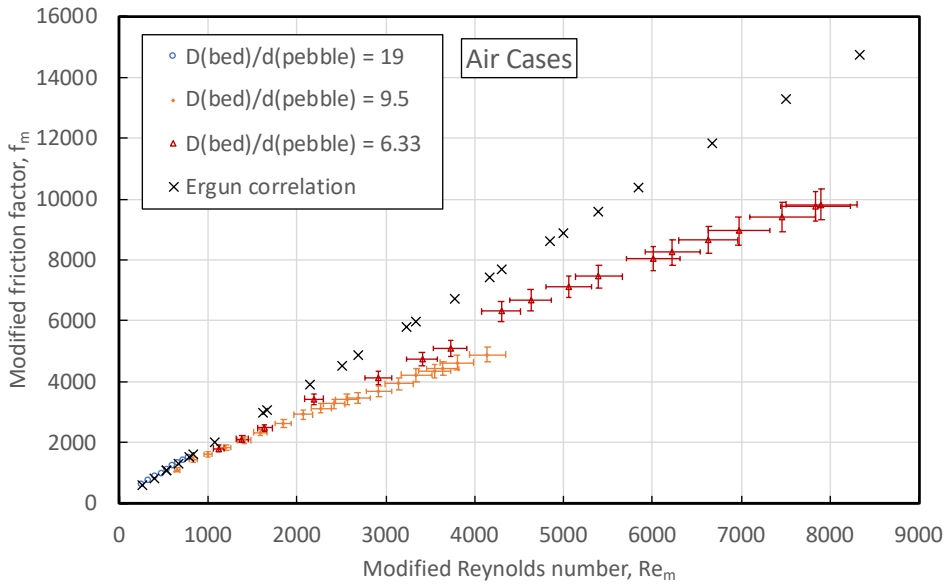

Figure 6 Comparison of SAM-predicted modified friction factor (f_m) between the Ergun correlation and TAMU air experimental measurements. Uncertainty of the Ergun correlation is not available and therefore not plotted. Uncertainties for experimental data are ±5.0% for Re_m, and ±5.1% for f_m, as reported in Hassan and Kang [6].

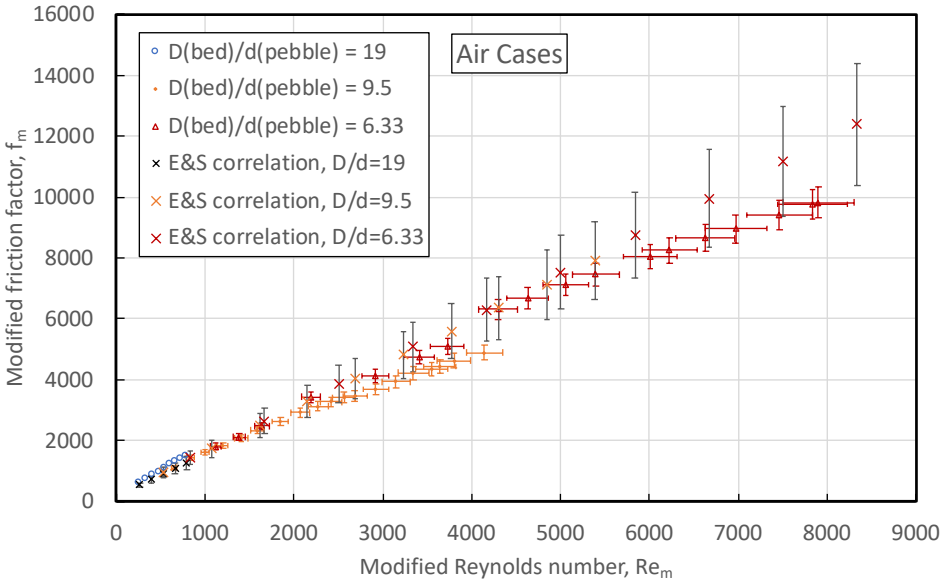

Figure 7 Comparison of SAM-predicted modified friction factor (f_m) between the Ergun correlation and TAMU air experimental measurements. A ±16.13% uncertainty bar is added for SAM-predicted results using the Eisfeld and Schnitzlein correlation. Uncertainties for experimental data are ±5.0% for Re_m and ±5.1% for f_m, as reported in Hassan and Kang [6].

4.2 Missouri S&T Air Experiments

A test facility was constructed at Missouri S&T to study the gas dynamics and heat transfer characteristics in a packed pebble bed for Gen-IV HTGRs [16]. Among investigated topics, the pressure drop through pebble beds is the main research objective of one of the separate-effect tests [16, 17].

The test facility of Missouri S&T for pressure drop tests consists of a Plexiglas column 0.3 m in diameter and 0.92 m in height. At the top of the pebble-bed column, a perforated distributor was installed to ensure uniform airflow from the upper plenum to the pebble column, and thus uniform inlet superficial velocity boundary conditions were assumed for all SAM simulations. At the bottom of the column, the pebble bed extended an additional 0.08 m beyond the bottom of the cylinder column to a cone-shaped volume, as shown in Figure 8. Such a test setup is susceptible to introducing nonuniformly distributed velocity and therefore pressure at the bottom of the column (marked as "interior surface" in Figure 8), as discussed later in this section. Three different sizes of pebbles, that is, diameter = 1.25, 2.5, and 5 cm, were used for randomly packing the bed, and the porosity of these beds was 0.375, 0.384, and 0.397, respectively. The dimensions of the test section are given in Table 4.

Table 4 Test section dimensions of Missouri S&T air pressure drop experiment

Bed height, L (m)	Bed diameter, D (m)	Particle diameter, d_p (cm)	D/d_p [-]	Bed porosity [-]
0.92	0.3	1.25	24	0.375
		2.5	12	0.384
		5.0	6	0.397

The Missouri S&T test used air as the working fluid and studied pressure drop in the pebble beds under different inlet superficial velocities, range 0.01–1.50 m/s, corresponding to modified Reynolds numbers, range ~10 to ~10^4. Abdullmohsin and Al-Dahhan [17] reported that pressure difference was measured between the inlet and outlet surface, as shown in Figure 8. However, experimental data and later SAM simulations results suggest that the "outlet" pressure was most likely measured at the bottom end of the cylinder column, that is, the "interior surface" marked in Figure 8. For all tests, fluid temperature was given as a fixed value, 21°C, but pressure was not given. As suggested by provided air properties (see Table B-1 of Appendix B), the outlet pressure is assumed to be at atmospheric pressure, 10^5 Pa.

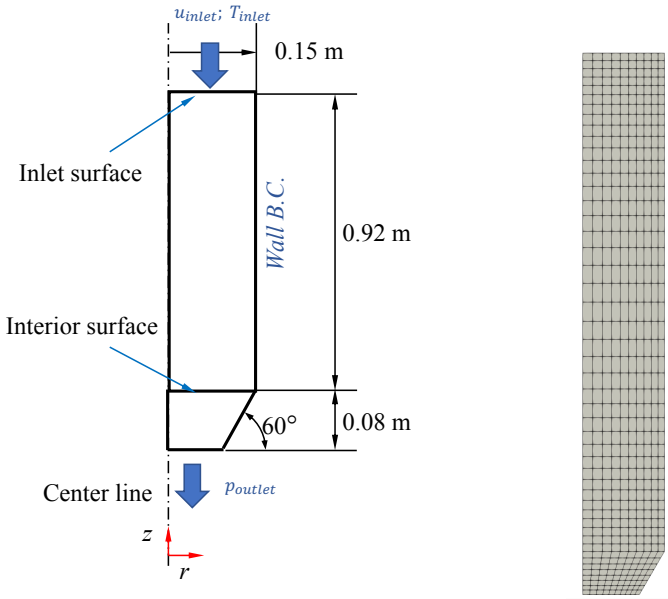

Figure 8 (left) Dimensions and boundary conditions setup for the Missouri S&T air test and (right) 2D-RZ mesh used for SAM simulation of Missouri S&T air test

Because of the large number of available test data, only part of them were used for this validation study; these are summarized in Table 4. Again, for simplicity, all simulations were performed using the 2D-RZ problem setup, and the boundary conditions were as shown in Figure 8. For each simulation, area-averaged pressures were obtained on the inlet surface and the interior surface, that is, p_{inlet} and p_{int}, and the frictional pressure drop was then computed as $p_{inlet} - p_{int} + \rho g H$ to compensate the gravity effect.

Table 5 Selected conditions for SAM simulations on Missouri S&T air test cases

Inlet superficial velocity (m/s)	Re_m		
	d_p = 5 cm D/d_p = 6	d_p = 2.5 cm D/d_p = 12	d_p = 1.25 cm D/d_p = 24
0.01	5.4401E+01	2.6626E+01	1.3121E+01
0.05	2.7200E+02	1.3313E+02	6.5607E+01
0.10	5.4401E+02	2.6626E+02	1.3121E+02
0.31	1.6864E+03	8.2541E+02	4.0676E+02
0.60	3.2640E+03	1.5976E+03	7.8728E+02
0.89	4.8416E+03	2.3697E+03	1.1678E+03
1.21	6.5825E+03	3.2218E+03	1.5877E+03
1.50	8.1601E+03	3.9939E+03	1.9682E+03

SAM-predicted non-dimensional drag coefficients were first compared with analytically computed values. Unlike the TAMU tests, the difference between SAM-predicted values and those from analytical expressions are not trivial. Although most of the differences are on the order of 0.1%, some differences are as large as 5% for small inlet velocities. Such deviations are caused by nonuniform velocity distribution near the bottom end of the porous bed because

of the existence of the cone-shaped outlet. As shown in Figure 9, it is very clear that velocity is nonuniform on the "interior" surface.

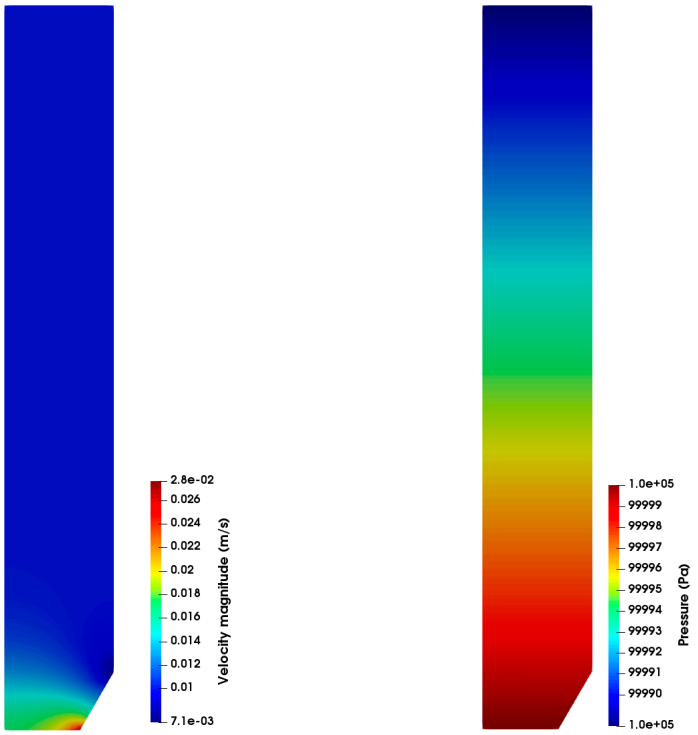

Figure 9 (left) Velocity magnitude distribution and (right) pressure distribution from SAM simulation results for inlet superficial velocity 0.01 m/s, d_p = 5 cm, using the KTA correlation

SAM-predicted non-dimensional drag coefficients are then compared with experimental measurements, as shown in Figure 10 to Figure 12:

- Figure 10 shows SAM results using the KTA correlation, which agree with experimental data very well over the entire modified Reynolds number range. All data points are well within the ±15% uncertainty bar, and most of the data points are within ±5% error.
- Figure 11 shows SAM results using the Ergun correlation. Although most data points are bounded with a ±20% error bar, the Ergun correlation starts to significantly overestimate the friction factor for larger Reynolds numbers.
- Figure 12 shows SAM results using the Eisfeld and Schnitzlein correlation, which also shows fairly good agreement with experimental data. All data points are within the correlation's ±16.13% uncertainty bar, with only two outlier points.

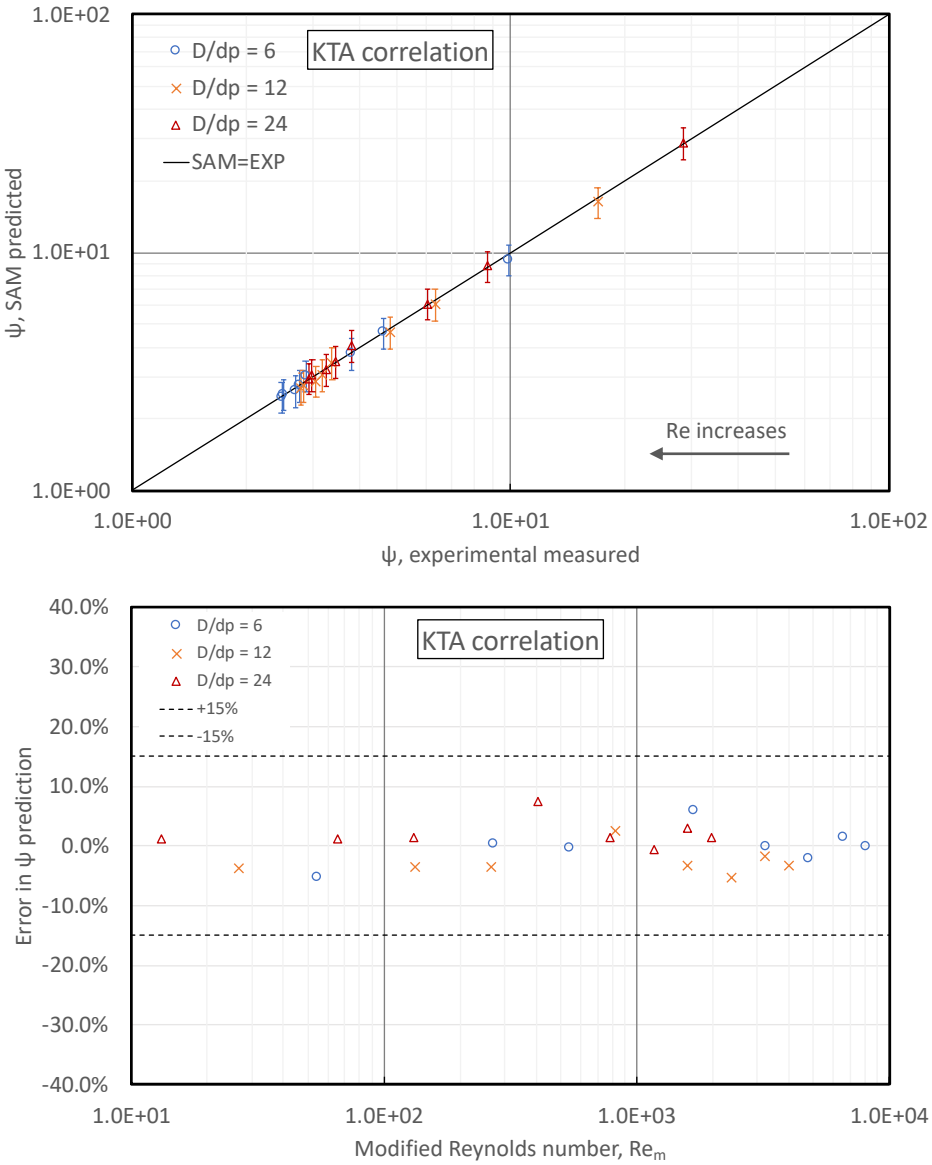

Figure 10 (top) Comparison of SAM-predicted non-dimensional drag coefficients between the KTA correlation and Missouri S&T experimental measurements and (bottom) prediction error plotted with modified Reynolds number. In both figures, a ±15% uncertainty bar is added for the KTA correlation.

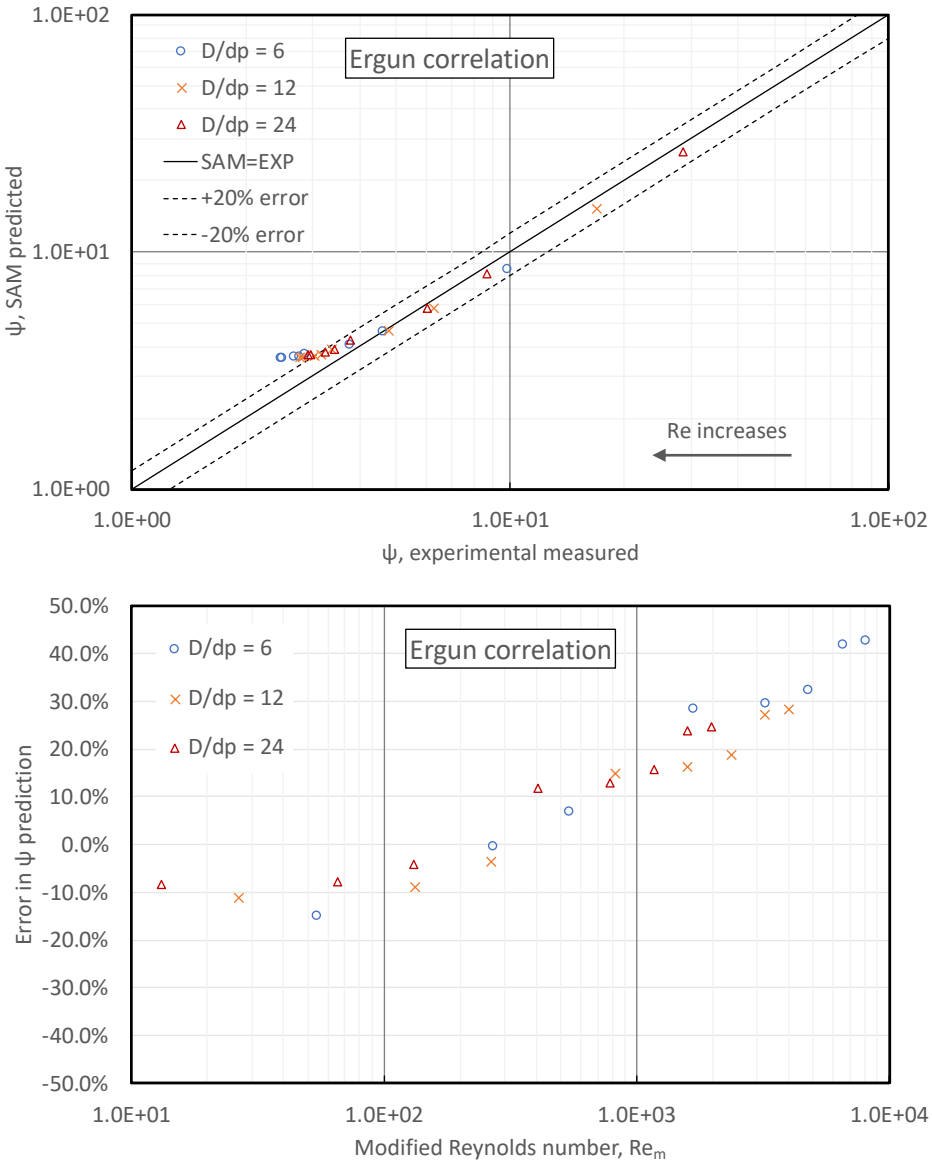

Figure 11 (top) Comparison of SAM-predicted non-dimensional drag coefficients between the Ergun correlation and Missouri S&T experimental measurements and (bottom) prediction error plotted with modified Reynolds number. In the top figure, a ±20% uncertainty bar is added for comparison, as Ergun correlation does not provide uncertainty information.

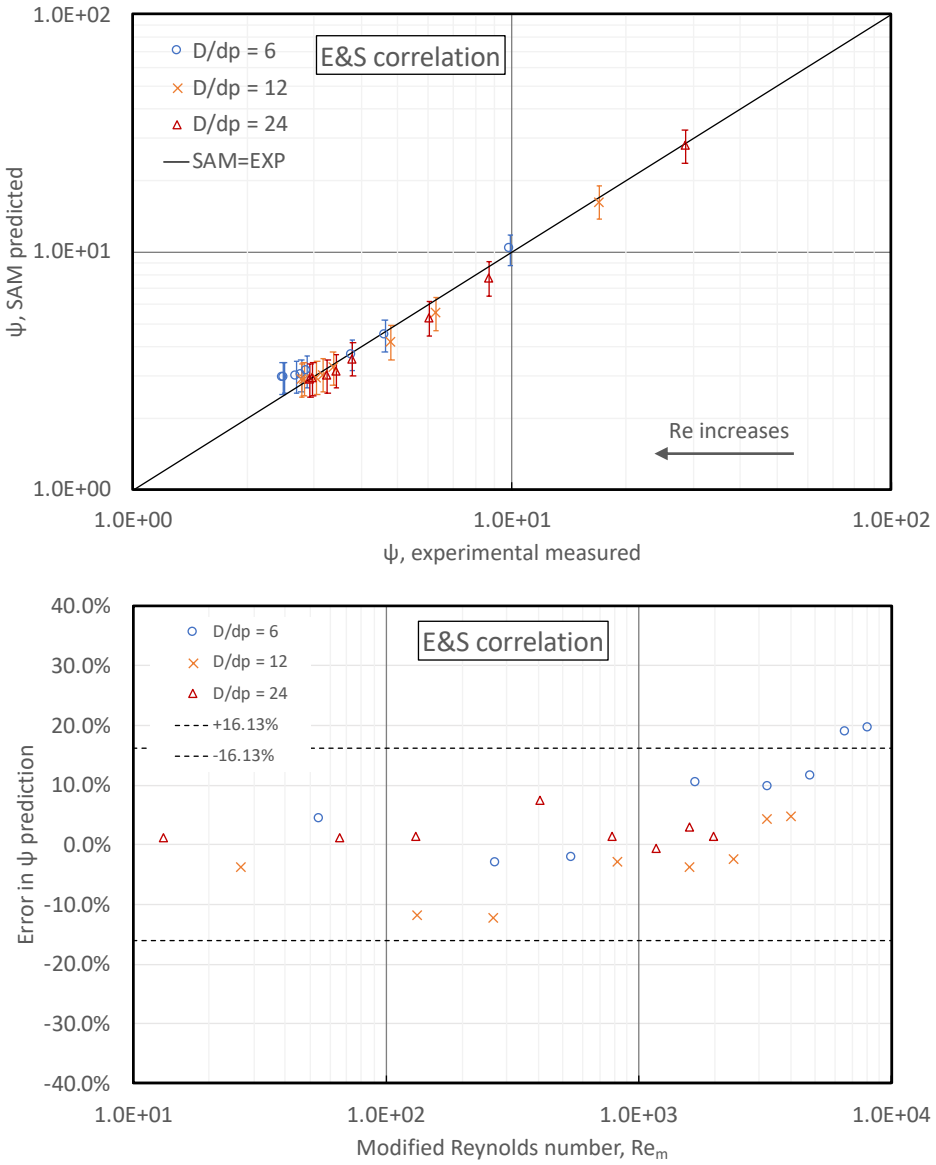

Figure 12 (top) Comparison of SAM-predicted non-dimensional drag coefficients between the Eisfeld and Schnitzlein correlation and Missouri S&T experimental measurements and (bottom) prediction error plotted with modified Reynolds number. In both figures, a ±16.13% uncertainty bar is added for the Eisfeld and Schnitzlein correlation.

4.3 North-West University Nitrogen Experiments

To support the Pebble Bed Modular Reactor (PBMR) technology development, the PBMR company, in cooperation with M-Tech Industrial (Pty) Ltd. and the North-West University of South Africa, has developed comprehensive separate and integral effects tests to study the various thermal-fluid phenomena essential to pebble-bed HTGRs [13]. This includes, for example, the non-nuclear high-temperature test unit (HTTU) [13, 14] and the high-pressure test unit (HPTU) [13, 14]. Experimental data from the HTTU test facility have been used in a

previous study to validate SAM code in predicting the effective thermal conductivity of packed pebble beds [5]. In the current work, the main focus is on validating SAM code for the frictional pressure drop across pebble beds using experimental data obtained from the HPTU tests.

The HPTU uses test sections of different packing configurations to investigate the frictional pressure drop across them, among many other test capabilities the test facility offers (see summary information in figure 16 in Rousseau and van Staden [13] and Table 3.1 of van der Walt [19]). With respect to pressure drop testing, the Pressure Drop Test Section (PDTS) provides a so-called "homogeneous porosity" pebble-bed configuration in which all pebbles are held in specific positions by using strings and are arranged in square columns. The positions of the strings and the space between pebbles could be adjusted to achieve different homogeneous porosity values. Such pebble-packing configurations are, however, not representative of realistic applications. Experimental data obtained from this test section were found to not be in reasonable agreement with any empirical correlations. For these reasons, the PDTS data were not used in this validation work.

The HPTU uses another two test sections with randomly packed pebble beds, namely, the small cylindrical packed bed (SCPB) and the small annular packed bed (SAPB). The dimensions of both test sections are scaled down from proposed PBMR cores, as summarized in Table 6, as well as depicted in Figure 13.

Table 6 Summary of the dimensions of the SCPB and SAPB test sections[a]

Test Section	Outer diameter (m)	Inner diameter (m)	Pebble bed height (m)	Porosity [-]	Pebble diameter (m)
SCPB	0.3689	-	0.1782	0.3967	6.002×10^{-3}
SAPB	0.3689	0.2	0.1788	0.3946	6.002×10^{-3}

[a] Data collected from Tables 3.1 and 4.3 of van der Walt [19].

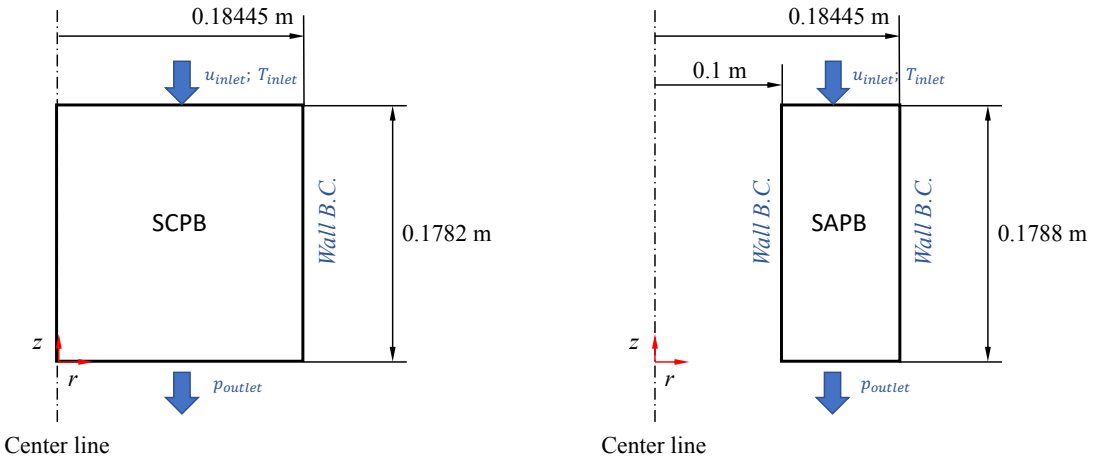

Figure 13 Dimensions and boundary conditions setup for the SCPB and SAPB tests

For code validation, SAM simulations were performed for all data points available from the experiment test matrix, that is, a list of predetermined Reynolds numbers and system pressures for both the SCPB and SAPB configurations. These data are summarized in the Table 7. Note

that for each test case, the modified Reynolds number and inlet superficial velocity are computed from given Reynolds number and fluid properties as function of system pressure and a constant temperature at 20°C.[2]

Table 7 Test matrix for SAM validation using SCPB and SAPB data[a]

Test number	Re	System pressure (MPa)	SCPB		SAPB	
			Re_m	Inlet superficial velocity (m/s)	Re_m	Inlet superficial velocity (m/s)
1	1000	0.309	1657.55	8.2574E-01	1651.80	8.2574E-01
2	2000	0.618	3315.10	8.2753E-01	3303.60	8.2753E-01
3	3000	0.928	4972.65	8.2846E-01	4955.40	8.2846E-01
4	4000	1.239	6630.20	8.2930E-01	6607.20	8.2930E-01
5	5000	1.552	8287.75	8.2966E-01	8259.00	8.2966E-01

[a] Reynolds numbers, Re, and system pressures are predetermined and therefore given. The modified Reynolds numbers, Re_m, are computed from Re and corresponding bed porosity, and inlet superficial velocities are computed as u = (Re μ)/(ρ d_p). Nitrogen densities and viscosities are given in Table C-1 in Appendix C.

For SAM simulations, we took advantage of the axisymmetric feature of both test sections, and all SAM simulations were performed using the 2D-RZ problem setup. For both SCPB and SAPB, uniformly distributed QUAD meshes, 10(R) × 40(Z), are used. For each simulation, inlet and outlet pressures, that is, p_{inlet} and p_{outlet}, are area-averaged pressure values of the inlet and outlet boundaries. Because of gravity effects, the total frictional pressure drop is computed as: $p_{inlet} - p_{outlet} + \rho g H$, in which H is the bed height. SAM-computed non-dimensional drag coefficients are provided in Table C-3 in Appendix C, and they agree with analytically computed values very well.

Comparisons between SAM-predicted results and experimental data are shown in Figure 14 for SCPB test cases and Figure 15 for SAPB test cases. For both the SCPB and SAPB test configurations, SAM-predicted results using both the KTA and the Eisfeld and Schnitzlein correlations show fairly good agreement with experimental data within their corresponding uncertainty ranges, for example, ±15% for the KTA correlation and ±16.13% for the Eisfeld and Schnitzlein correlation. The Ergun correlation again overestimates the non-dimensional drag coefficient for all cases, with errors in the range ~15% to 35%.

[2]This value is based on the discussion provided in section 4.3.1 of van der Walt [19]. As a matter of fact, temperature and pressure won't affect validation results, as the comparisons are based on non-dimensional numbers, that is, modified Reynolds number versus non-dimensional drag coefficient.

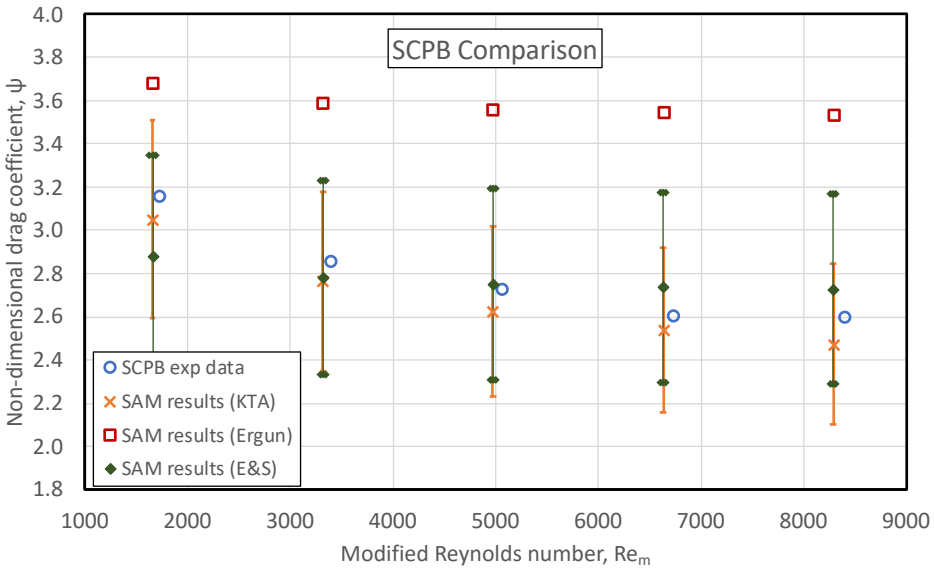

Figure 14 Comparison between SAM-predicted non-dimensional drag coefficients and SCPB experimental measurements. A ±15% uncertainty bar is added for SAM-predicted results using the KTA correlation; a ±16.13% uncertainty bar for the Eisfeld and Schnitzlein correlation; and no uncertainty bar for the Ergun correlation. Reported uncertainty range for SCPB data is about ±16.24% (not shown). Small uncertainties in Reynolds number are also evident in van der Walt [19], also not shown.

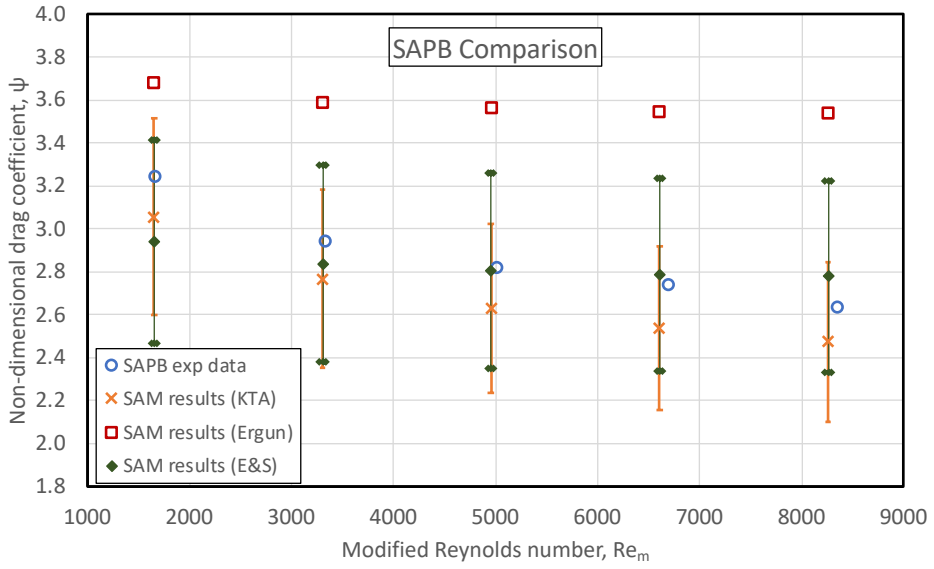

Figure 15 Comparison between SAM-predicted non-dimensional drag coefficients and SAPB experimental measurements. A ±15% uncertainty bar is added for SAM-predicted results using the KTA correlation; a ±16.13% uncertainty bar for the Eisfeld and Schnitzlein correlation; and no uncertainty bar for the Ergun correlation. Reported uncertainty range for SCPB data is about ±17.8% (not shown). Small uncertainties in Reynolds number are also evident in van der Walt [19], also not shown.

5 Summary

This report summarizes a recent effort to validate the capability of SAM code to predict the frictional pressure drop through pebble beds using selected experimental data, including those obtained from test facilities at TAMU, Missouri S&T, and North-West University of South Africa. Currently, SAM implements three empirical correlations to predict the frictional pressure drop: the classical Ergun correlation; the KTA correlation, which is widely used in HTGR applications; and the Eisfeld and Schnitzlein correlation, which explicitly considers wall effects. When possible, verification was also performed to compare SAM-predicted values with those computed from analytical expressions. For all selected experimental data, the KTA correlation shows the best performance and agree very well with experimental measurement. For all most all data points (except for the small D/d_p ratio of TAMU water test), the KTA correlation was able to match experimental data within its uncertainty range, ±15%. The Eisfeld and Schnitzlein correlation also shows quite good accuracy over the entire modified Reynolds number range within its uncertainty range ±16.13%, although it tends to overpredict pressure drop for larger Reynolds numbers. In addition, for experimental data investigated in this report, there is no evidence to show that the Eisfeld and Schnitzlein correlation is better than the KTA correlation, although it explicitly considers the wall effect. Overall, the Ergun correlation tends to overpredict frictional pressure drop for almost all studied data points, except for small modified Reynolds numbers, i.e., <1000. This might be due to the limit Reynolds number range data points used to fit the Ergun correlation.

Overall, this report presents a successful effort to validate SAM's capability to predict frictional pressure drop through porous pebble beds. Further code development and validation efforts will be performed to continue to enhance SAM code capability in other areas related to pebble-bed reactor analysis, including, for example, convective heat transfer between coolant and pebble beds.

6 Acknowledgment

This report was prepared as an account of work sponsored by an agency of the U.S. Government. Neither the U.S. Government nor any agency thereof, nor any of their employees, makes any warranty, expressed or implied, or assumes any legal liability or responsibility for any third party's use, or the results of such use, of any information, apparatus, product, or process disclosed in this report, or represents that its use by such third party would not infringe privately owned rights. The views expressed in this paper are not necessarily those of the U.S. Nuclear Regulatory Commission.

This work is supported by the U.S. Nuclear Regulatory Commission, under Task Order Agreement No. NRC-HQ-25-14-D-0003. The authors sincerely thank Mr. Joseph Kelly at the U.S. Nuclear Regulatory Commission for providing suggestions on experimental data selection and Missouri S&T pressure drop experimental data.

7 References

[1] Z. Gao and L. Shi, Thermal Hydraulic Calculation of the HTR-10 for the Initial and Equilibrium Ccore, *Nuclear Engineering and Design*, 218:51–64, 2002.

[2] Y. Zheng, L. Shi, and Y. Dong, Thermohydraulic Transient Studies of the Chinese 200 MWe HTR-PM for Loss of Forced Cooling Accidents, *Annals of Nuclear Energy*, 36:742–751, 2009.

[3] R. Hu, *SAM Theory Manual*, Technical Report ANL/NE-17/4, Argonne National Laboratory, , Lemont, IL, March 2017.

[4] U.S. Nuclear Regulatory Commission, NRC Non-Light Water Reactor (Non-LWR) Vision and Strategy, Vol. 1 – Computer Code Suite for Non-LWR Plant Systems Analysis. Rev. 1, Technical Report, U.S. NRC, January 31, 2020.

[5] L. Zou and R. Hu, *Recent SAM Code Improvement to Heat Transfer Modeling Capabilities*, Technical Report ANL/NSE-19/46, Argonne National Laboratory, Lemont, IL, December 2019.

[6] Y. A. Hassan and C. Kang, Pressure Drop in a Pebble Bed Reactor under High Reynolds Number, *Nuclear Technology*, 180(2):159–173, 2012.

[7] R. Hu, Three-Dimensional Flow Model Development for thermal Mixing and Stratification Modeling in Reactor System Transients Analyses, *Nuclear Engineering and Design*, 345:209–215, 2019.

[8] F. C. Blake, The Resistance of Packing to Fluid Flow, *Transactions of American Institute of Chemical Engineers*, 14:415–421, 1922.

[9] S. Ergun, Fluid Flow through Packed Columns, *Chemical Engineering Progress*, 48(2):89–94, 1952.

[10] Fenech, H., (Ed.), *Heat Transfer and Fluid Flow in Nuclear Systems*, Pergamon Press, 1981.

[11] Nuclear Safety Standards Commission, Reactor Core Design of High-Temperature Gas-Cooled Reactors; Part3: Loss of Pressure through Friction in Pebble Bed Cores, Technical Report KTA 3102.3, 1981.

[12] B. Eisfeld and K. Schnitzlein, The Influence of Confining Walls on the Pressure Drop in Packed Beds, *Chemical Engineering Science*, 56:4321–329, 2001.

[13] P. G. Rousseau and M. van Staden, Introduction to the PBMR Heat Transfer Test Facility, *Nuclear Engineering and Design*, 238(11):3060–3072, 2008.

[14] P. G. Rousseau, C. G. du Toit, W. van Antwerpen, and H. J. van Antwerpen, Separate Effects Tests to Determine the Effective Thermal Conductivity in the PBMR HTTU Test Facility, *Nuclear Engineering and Design*, 271:444–458, 2014.

[15] C.W. Kang, Pressure Drop in a Pebble Bed Reactor, Master's Thesis, Texas A&M University, August 2010.

[16] R. Abdullmohsin, Gas Dynamics and Heat Transfer in a Packed Pebble-Bed Reactor for the 4th Generation Nuclear Eenergy, Doctoral Dissertation, Missouri University of Science and Technology, Fall 2013.

[17] R. Abdullmohsin and M. H. Al-Dahhan, Pressure Drop and Fluid Flow Characteristics in a Packed Pebble Bed Reactor, *Nuclear Technology*, 198:17–25, 2017.

[18] National Institute of Standards and Technology, *NIST Chemistry WebBook*, SRD 69. Available at https://webbook.nist.gov. Accessed Feb. 10, 2020.

[19] AJK van der Walt, Pressure Drop through a Packed Bed, Master's Thesis, North-West University, December 2006.

Appendix A: Supplemental Data/Results for TAMU Validation

A.1 Water and Air Properties

Table A-1 Water properties used for TAMU test validation, obtained from NIST [18].

Temperature (°C)	Pressure (bar)	Density (kg/m^3)	Viscosity (Pa·s)
30	1	995.65	797.35e-6

Table A-2 Air properties used for TAMU test validation, provided in Kang [15]

Temperature (°C)	Pressure (bar)	Density (kg/m^3)	Viscosity (Pa·s)
-	-	1.1726	1.83538e-5

A.2 TAMU Experimental Data

Table A-3 Experimental data used for TAMU tests validation: Water with vertical test section configuration, provided in the appendix of Kang [15]

d_p = 6.35 mm		d_p = 12.7 mm		d_p = 19.05 mm		d_p = 33.02 mm	
Re_m	f_m	Re_m	f_m	Re_m	f_m	Re_m	f_m
899.47	1794	3165	4579	6324	8779	20047	17184
1060.77	2022	3542	5037	6915	9475	22512	19203
1258.2	2301	3888	5425	8132	10700	24933	21379
1641.35	2827	4455	6047	9374	11963	27371	23365
1794.39	3003	4622	6190	10578	13280	29936	25646
2222.33	3603	4984	6588	11749	14639		
2361.01	3758	5340	6983	12908	16024		
2802.3	4339	6005	7685	14013	17220		
2988.53	4556	6068	7755				
3354.77	5014	6422	8146				
		6796	8497				
		7522	9311				
		7492	9259				
		7866	9730				
		8172	10022				

Table A-4 Experimental data used for TAMU tests validation: Water with horizontal test section configuration, provided in the appendix of Kang [15]

d_p = 6.35 mm		d_p = 12.7 mm		d_p = 19.05 mm		d_p = 33.02 mm	
Re_m	f_m	Re_m	f_m	Re_m	f_m	Re_m	f_m
518.0825	1171.5105	2524	3690.47	4667	6159	18721	16440
661.6456	1333.5559	2947	4352.77	5205	6763	19725	16907
850.5672	1579.0364	2941	4185.39	5753	7434	21049	18266
938.6135	1634.0506	3397	4742.83	6641	8730	22036	18996
1191.1256	1994.6389	4087	5752.56	7832	9993	23319	20033
1450.0716	2290.3866	4848	6560.41	9023	11140	24322	20854
1718.1952	2628.5581	5727	7516.34	10046	12352	25551	22070
1976.1965	2952.6902	6524	8374.91	11379	13855	26676	22808
2225.2683	3265.0175	7436	9321.96	12024	14677	27938	23894
2474.2467	3557.1122	8161	10091.18	13920	16751		
2674.154	3800.2483	9008	11082.89				
2836.0785	3971.6019	9283	11355.45				

Table A-5 Experimental data used for TAMU tests validation: Air with horizontal test section configuration, provided in the appendix of Kang [15]

d_p = 6.35 mm		d_p = 12.7 mm		d_p = 19.05 mm	
Re_m	f_m	Re_m	f_m	Re_m	f_m
263	617	647	1106	1118	1811
336	742	836	1434	1381	2122
409	847	1000	1613	1634	2478
478	952	1201	1846	2193	3437
542	1080	1404	2081	2917	4135
603	1204	1590	2333	3406	4743
670	1309	1848	2634	3727	5086
732	1405	2071	2920	4296	6314
793	1503	2268	3133	4631	6674
		2418	3272	5055	7113
		2562	3403	5396	7457
		2683	3467	6005	8053
		2921	3692	6224	8263
		3148	3938	6633	8650
		3344	4229	6968	8964
		3551	4357	7462	9419
		3645	4424	7833	9758
		3798	4626	7902	9821
		4142	4891		

A.3 SAM Simulations Results and Analytical Values

Table A-6 SAM simulation results for selected Reynolds number conditions for TAMU water tests

		KTA		Ergun		Eisfeld and Schnitzlein	
u_{inlet}	Re_m	f_m (analytical)	f_m (SAM results)	f_m (analytical)	f_m (SAM results)	f_m (analytical)	f_m (SAM results)
d_p = 6.35 mm; D/d_p = 19							
0.05	6.4465E+02	1.1728E+03	1.1728E+03	1.2781E+03	1.2781E+03	1.0658E+03	1.0658E+03
0.1	1.2893E+03	2.0499E+03	2.0499E+03	2.4063E+03	2.4063E+03	1.9595E+03	1.9595E+03
0.2	2.5786E+03	3.6867E+03	3.6867E+03	4.6626E+03	4.6626E+03	3.7470E+03	3.7470E+03
0.25	3.2233E+03	4.4711E+03	4.4711E+03	5.7907E+03	5.7907E+03	4.6408E+03	4.6408E+03
d_p = 12.7 mm; D/d_p = 9.5							
0.1	2.6299E+03	3.7498E+03	3.7498E+03	4.7524E+03	4.7524E+03	3.9597E+03	3.9597E+03
0.2	5.2599E+03	6.8588E+03	6.8588E+03	9.3548E+03	9.3547E+03	7.7275E+03	7.7275E+03
0.3	7.8898E+03	9.8090E+03	9.8090E+03	1.3957E+04	1.3957E+04	1.1495E+04	1.1495E+04
0.4	1.0520E+04	1.2660E+04	1.2660E+04	1.8560E+04	1.8560E+04	1.5263E+04	1.5263E+04
d_p = 19.05 mm; D/d_p = 6.33							
0.1	4.0732E+03	5.4819E+03	5.4819E+03	7.2782E+03	7.2782E+03	6.1672E+03	6.1672E+03
0.2	8.1465E+03	1.0091E+04	1.0091E+04	1.4406E+04	1.4406E+04	1.2120E+04	1.2120E+04
0.3	1.2220E+04	1.4465E+04	1.4465E+04	2.1535E+04	2.1535E+04	1.8073E+04	1.8073E+04
0.4	1.6293E+04	1.8692E+04	1.8692E+04	2.8663E+04	2.8663E+04	2.4025E+04	2.4025E+04
d_p = 33.02 mm; D/d_p = 3.65							
0.1	7.7069E+03	9.6074E+03	9.6073E+03	1.3637E+04	1.3637E+04	1.1582E+04	1.1582E+04
0.2	1.5414E+04	1.7790E+04	1.7790E+04	2.7124E+04	2.7124E+04	2.2887E+04	2.2887E+04
0.3	2.3121E+04	2.5554E+04	2.5554E+04	4.0611E+04	4.0611E+04	3.4193E+04	3.4193E+04
0.4	3.0828E+04	3.3058E+04	3.3058E+04	5.4098E+04	5.4098E+04	4.5498E+04	4.5498E+04

Table A-7 SAM simulation results for selected Reynolds number conditions for TAMU air tests

		KTA		Ergun		Eisfeld and Schnitzlein	
u_{inlet}	Re_m	f_m (analytical)	f_m (SAM results)	f_m (analytical)	f_m (SAM results)	f_m (analytical)	f_m (SAM results)
d_p = 6.35 mm; D/d_p = 19							
0.4	2.6387E+02	6.1328E+02	6.1325E+02	6.1176E+02	6.1179E+02	5.3789E+02	5.3789E+02
0.6	3.9580E+02	8.1290E+02	8.1289E+02	8.4265E+02	8.4265E+02	7.2080E+02	7.2081E+02
0.8	5.2773E+02	1.0058E+03	1.0059E+03	1.0735E+03	1.0735E+03	9.0371E+02	9.0370E+02
1	6.5966E+02	1.1940E+03	1.1940E+03	1.3044E+03	1.3044E+03	1.0866E+03	1.0866E+03
1.2	7.9160E+02	1.3784E+03	1.3784E+03	1.5353E+03	1.5353E+03	1.2695E+03	1.2695E+03
d_p = 12.7 mm; D/d_p = 9.5							
0.4	5.3823E+02	1.0210E+03	1.0211E+03	1.0919E+03	1.0920E+03	9.6303E+02	9.6301E+02
0.8	1.0765E+03	1.7667E+03	1.7666E+03	2.0338E+03	2.0338E+03	1.7341E+03	1.7341E+03
1.2	1.6147E+03	2.4742E+03	2.4742E+03	2.9757E+03	2.9758E+03	2.5052E+03	2.5053E+03
1.6	2.1529E+03	3.1581E+03	3.1581E+03	3.9176E+03	3.9176E+03	3.2763E+03	3.2764E+03
2.0	2.6912E+03	3.8249E+03	3.8249E+03	4.8595E+03	4.8595E+03	4.0475E+03	4.0475E+03
2.4	3.2294E+03	4.4785E+03	4.4785E+03	5.8014E+03	5.8014E+03	4.8186E+03	4.8185E+03
2.8	3.7676E+03	5.1212E+03	5.1211E+03	6.7434E+03	6.7433E+03	5.5897E+03	5.5897E+03
3.2	4.3059E+03	5.7547E+03	5.7547E+03	7.6853E+03	7.6853E+03	6.3608E+03	6.3608E+03
3.6	4.8441E+03	6.3803E+03	6.3803E+03	8.6272E+03	8.6272E+03	7.1319E+03	7.1319E+03
4.0	5.3823E+03	6.9990E+03	6.9990E+03	9.5691E+03	9.5691E+03	7.9030E+03	7.9030E+03
d_p = 19.05 mm; D/d_p = 6.33							
0.4	8.3362E+02	1.4364E+03	1.4364E+03	1.6088E+03	1.6089E+03	1.4328E+03	1.4330E+03
0.8	1.6672E+03	2.5419E+03	2.5418E+03	3.0677E+03	3.0676E+03	2.6510E+03	2.6510E+03
1.2	2.5008E+03	3.5908E+03	3.5908E+03	4.5265E+03	4.5265E+03	3.8693E+03	3.8692E+03
1.6	3.3345E+03	4.6047E+03	4.6047E+03	5.9853E+03	5.9853E+03	5.0875E+03	5.0875E+03
2.0	4.1681E+03	5.5933E+03	5.5932E+03	7.4441E+03	7.4441E+03	6.3058E+03	6.3058E+03
2.4	5.0017E+03	6.5622E+03	6.5622E+03	8.9030E+03	8.9029E+03	7.5240E+03	7.5240E+03
2.8	5.8353E+03	7.5149E+03	7.5149E+03	1.0362E+04	1.0362E+04	8.7423E+03	8.7423E+03
3.2	6.6689E+03	8.4541E+03	8.4541E+03	1.1821E+04	1.1821E+04	9.9605E+03	9.9606E+03
3.6	7.5025E+03	9.3817E+03	9.3816E+03	1.3279E+04	1.3279E+04	1.1179E+04	1.1179E+04
4.0	8.3362E+03	1.0299E+04	1.0299E+04	1.4738E+04	1.4738E+04	1.2397E+04	1.2397E+04

A.4 Zoom-in View of SAM Correlations versus Experimental Data

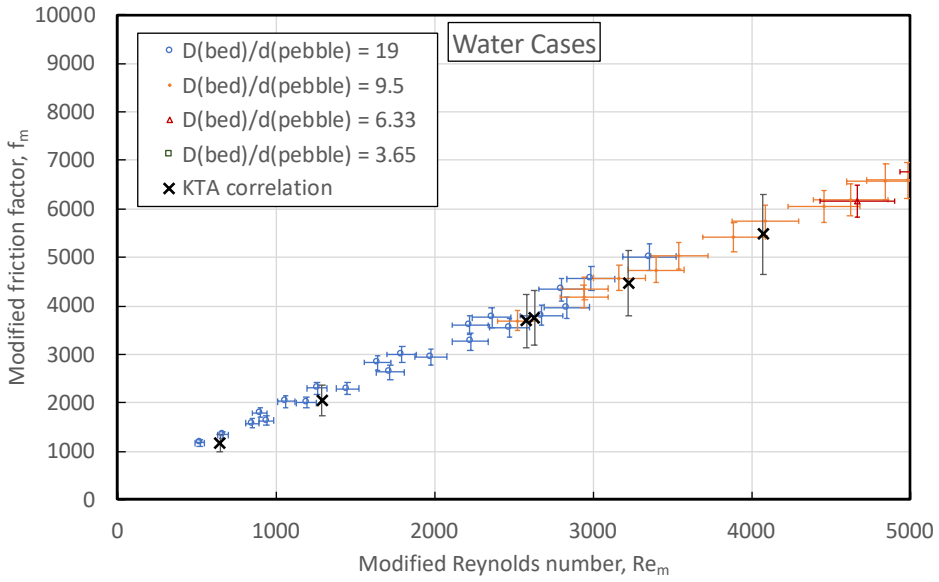

Figure A-1 Comparison of SAM-predicted modified friction factor (f_m) between the KTA correlation and TAMU water experimental measurements: Zoom-in view for Re_m between 0 and 5000

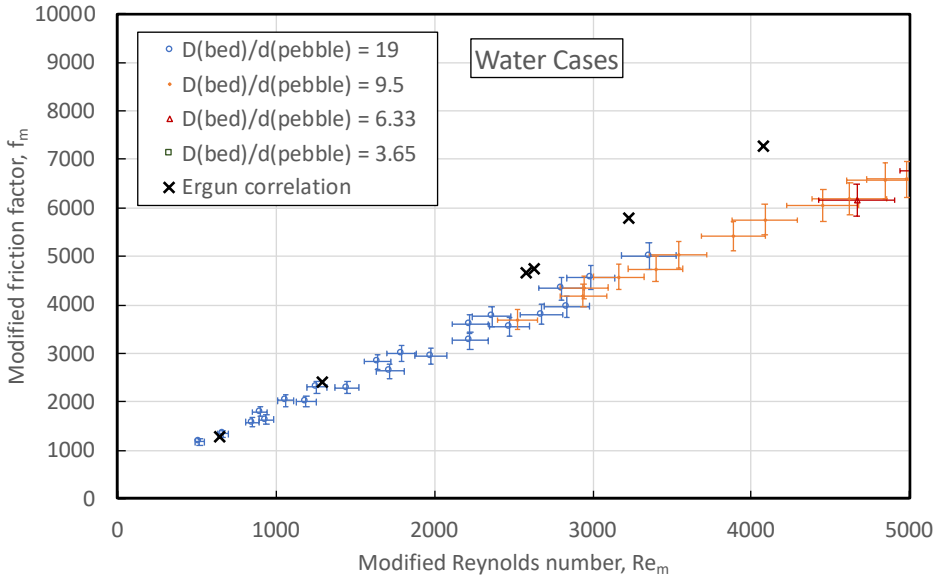

Figure A-2 Comparison of SAM-predicted modified friction factor (f_m) between the Ergun correlation and TAMU water experimental measurements: Zoom-in view for Re_m between 0 and 5000

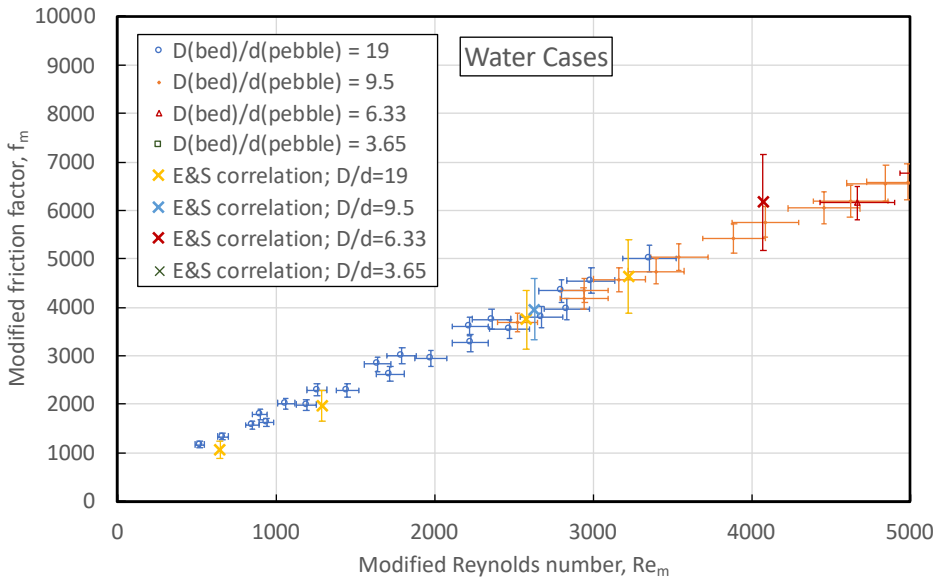

Figure A-3 Comparison of SAM-predicted modified friction factor (f_m) between the Eisfeld and Schnitzlein correlation and TAMU water experimental measurements: Zoom-in view for Re_m between 0 and 5000

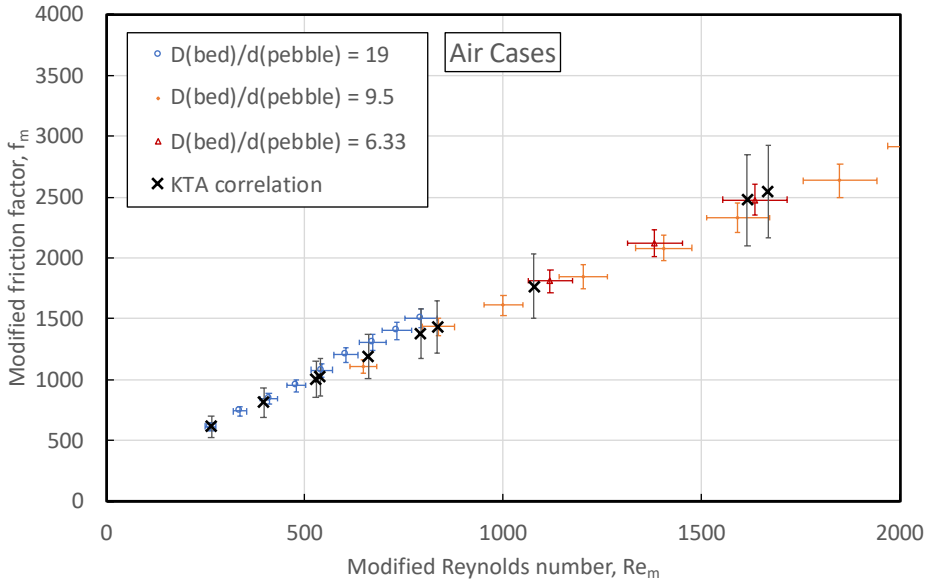

Figure A-4 Comparison of SAM-predicted modified friction factor (f_m) between the KTA correlation and TAMU air experimental measurements: Zoom-in view for Re_m between 0 and 2000

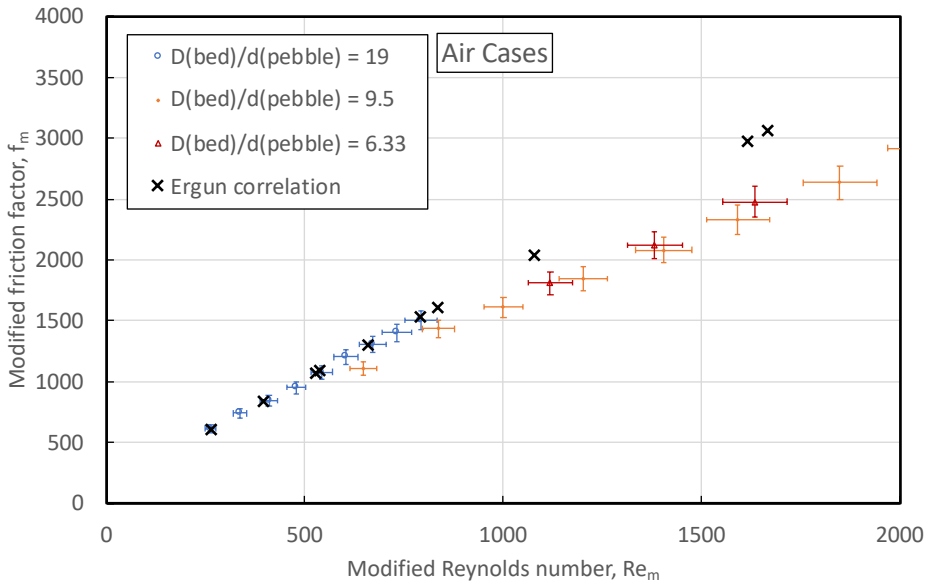

Figure A-5 Comparison of SAM-predicted modified friction factor (f_m) between the Ergun correlation and TAMU air experimental measurements: Zoom-in view for Re_m between 0 and 2000.

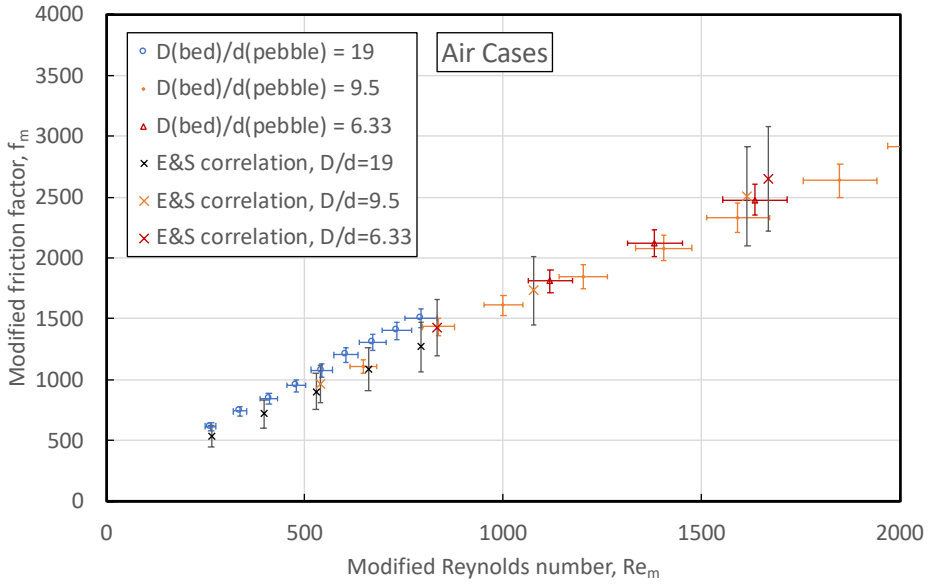

Figure A-6 Comparison of SAM-predicted modified friction factor (f_m) between the Eisfeld and Schnitzlein correlation and TAMU air experimental measurements: Zoom-in view for Re_m between 0 and 2000

Appendix B: Supplemental Data/Results for Missouri S&T Validation

B.1 Air Properties

Table B-1 Air properties provided and used in the Missouri S&T experiment validation

Temperature (°C)	Pressure	Density (kg/m^3)	Viscosity (Pa·s)
21	Not given, assumed to be atmospheric pressure, 10^5 Pa	1.187711	1.8E-05

B.2 Missouri S&T Experimental Data

Table B-2 Raw experimental data of Missouri S&T air tests

Superficial velocity (m/s)	Pressure drop, ΔP (kPa)		
	$(D/d_p) = 6$	$(D/d_p) = 12$	$(D/d_p) = 24$
0.01	0.000104	0.0004037	0.0014814
0.03	0.000529	0.0017495	0.005645
0.05	0.001215	0.00375	0.0112683
0.08	0.002707	0.0079068	0.022281
0.10	0.003998	0.0114205	0.0312782
0.12	0.00552	0.0155122	0.0415643
0.15	0.008227	0.022711	0.0593597
0.20	0.013843	0.0374729	0.0951812
0.24	0.020806	0.0556061	0.1385198
0.31	0.029087	0.0770358	0.189208
0.40	0.049509	0.1295543	0.3121219
0.49	0.07496	0.1946551	0.4630906
0.60	0.105327	0.2720582	0.6414893
0.71	0.140521	0.3615398	0.8468193
0.81	0.180468	0.4629143	1.0786668
0.89	0.225105	0.576023	1.3366789
1.00	0.274377	0.7007297	1.6205486
1.10	0.328234	0.836911	1.9300042
1.21	0.386634	0.9844585	2.2648026
1.30	0.449536	1.143273	2.6247241
1.41	0.516906	1.3132658	3.0095679
1.50	0.58871	1.4943532	3.41915

B.3 SAM Simulation Results for Selected Missouri S&T Data Points

Table B-3 Comparison between SAM predictions and experimental data for selected cases for $(D/d_p) = 6$

Superficial velocity (m/s)	Re_m	Ψ_{exp}	SAM results, KTA		SAM results, Ergun		SAM results, E&S	
			Ψ_{SAM}	Error	Ψ_{SAM}	Error	Ψ_{SAM}	Error
0.01	5.4401E+01	9.8762E+00	9.3443E+00	-5.3855E-02	8.3947E+00	-1.5001E-01	1.0294E+01	4.2299E-02
0.05	2.7200E+02	4.6167E+00	4.6281E+00	2.4697E-03	4.5901E+00	-5.7581E-03	4.4762E+00	-3.0441E-02
0.10	5.4401E+02	3.7963E+00	3.7780E+00	-4.8031E-03	4.0534E+00	6.7740E-02	3.7115E+00	-2.2314E-02
0.31	1.6864E+03	2.8743E+00	3.0444E+00	5.9171E-02	3.6867E+00	2.8264E-01	3.1729E+00	1.0386E-01
0.60	3.2640E+03	2.7784E+00	2.7753E+00	-1.1260E-03	3.5983E+00	2.9509E-01	3.0496E+00	9.7614E-02
0.89	4.8416E+03	2.6987E+00	2.6376E+00	-2.2642E-02	3.5692E+00	3.2253E-01	3.0069E+00	1.1418E-01
1.21	6.5825E+03	2.5078E+00	2.5426E+00	1.3901E-02	3.5525E+00	4.1661E-01	2.9830E+00	1.8952E-01
1.50	8.1601E+03	2.4847E+00	2.4805E+00	-1.7011E-03	3.5436E+00	4.2618E-01	2.9705E+00	1.9551E-01

Table B-4 Comparison between SAM predictions and experimental data for selected cases for $(D/d_p) = 12$

Superficial velocity (m/s)	Re_m	Ψ_{exp}	SAM results, KTA		SAM results, Ergun		SAM results, E&S	
			Ψ_{SAM}	Error	Ψ_{SAM}	Error	Ψ_{SAM}	Error
0.01	2.6626E+01	1.6978E+01	1.6337E+01	-3.7783E-02	1.5075E+01	-1.1210E-01	1.6337E+01	-3.7783E-02
0.05	1.3313E+02	6.3092E+00	6.0878E+00	-3.5083E-02	5.7513E+00	-8.8417E-02	5.5662E+00	-1.1775E-01
0.10	2.6626E+02	4.8036E+00	4.6303E+00	-3.6082E-02	4.6303E+00	-3.6082E-02	4.2097E+00	-1.2364E-01
0.31	8.2541E+02	3.3717E+00	3.4537E+00	2.4309E-02	3.8695E+00	1.4763E-01	3.2742E+00	-2.8913E-02
0.60	1.5976E+03	3.1787E+00	3.0729E+00	-3.3264E-02	3.6945E+00	1.6228E-01	3.0624E+00	-3.6572E-02
0.89	2.3697E+03	3.0588E+00	2.8962E+00	-5.3148E-02	3.6332E+00	1.8781E-01	2.9875E+00	-2.3288E-02
1.21	3.2218E+03	2.8282E+00	2.7772E+00	-1.8030E-02	3.5997E+00	2.7279E-01	2.9473E+00	4.2104E-02
1.50	3.9939E+03	2.7935E+00	2.7013E+00	-3.3021E-02	3.5820E+00	2.8223E-01	2.9253E+00	4.7148E-02

Table B-5 Comparison between SAM predictions and experimental data for selected cases for $(D/d_p) = 24$

Superficial velocity (m/s)	Re_m	Ψ_{exp}	SAM results, KTA		SAM results, Ergun		SAM results, E&S	
			Ψ_{SAM}	Error	Ψ_{SAM}	Error	Ψ_{SAM}	Error
0.01	1.3121E+01	2.8598E+01	2.8926E+01	1.1446E-02	2.6223E+01	-8.3057E-02	2.8153E+01	1.1446E-02
0.05	6.5607E+01	8.7011E+00	8.8093E+00	1.2430E-02	8.0371E+00	-7.6314E-02	7.8054E+00	1.2430E-02
0.10	1.3121E+02	6.0381E+00	6.1211E+00	1.3753E-02	5.7929E+00	-4.0598E-02	5.3103E+00	1.3753E-02
0.31	4.0676E+02	3.8008E+00	4.0800E+00	7.3466E-02	4.2447E+00	1.1680E-01	3.5778E+00	7.3466E-02
0.60	7.8728E+02	3.4399E+00	3.4904E+00	1.4683E-02	3.8893E+00	1.3066E-01	3.1783E+00	1.4683E-02
0.89	1.1678E+03	3.2576E+00	3.2387E+00	-5.8133E-03	3.7656E+00	1.5593E-01	3.0403E+00	-5.8133E-03
1.21	1.5877E+03	2.9862E+00	3.0769E+00	3.0380E-02	3.6977E+00	2.3826E-01	2.9646E+00	3.0380E-02
1.50	1.9682E+03	2.9335E+00	2.9769E+00	1.4787E-02	3.6613E+00	2.4809E-01	2.9238E+00	1.4787E-02

Appendix C: Supplemental Data/Results for North-West University of South Africa Validation

C.1 Nitrogen Properties

Nitrogen properties have been obtained from NIST [18], and they are given in Table C-1. Nitrogen properties are also available and are provided as fitted curves in van der Walt [19]; however, they were not used in this validation study.

Table C-1 Nitrogen properties obtained from NIST [18]

Temperature (°C)	Pressure (MPa)	Density (kg/m^3)	Viscosity (Pa·s)
20	0.309	3.554	1.7614E-05
20	0.618	7.1128	1.7664E-05
20	0.928	10.688	1.7715E-05
20	1.239	14.278	1.7767E-05
20	1.552	17.894	1.7821E-05

C.2 SCPB and SAPB Experimental Data

SCPB and SAPB experimental data are digitalized from figure 5.10 of van der Walt [19]. This process inevitably introduces additional errors; however, it is believed this additional uncertainty is very small compared to experimental uncertainties. Digitalized SCPB and SAPB experimental data are given in Table C-2. Also, the non-dimensional drag coefficient given in Table C-2 is twice the friction factor value given in figure 5.10 of van der Walt [19], since a different non-dimensional factor was used in this study.

Table C-2 Digitalized SCPB and SAPB experimental data from van der Walt [19]

SCPB		SAPB	
Re_m	Nondimensional drag coefficient, Ψ	Re_m	Nondimensional drag coefficient, Ψ
1715	3.16	1660	3.244
3386	2.86	3335	2.94
5052	2.732	5011	2.82
6725	2.606	6686	2.74
8395	2.6	8353	2.634

C.3 SCPB and SAPB SAM Results Compared with Analytical Values

Table C-3 SAM-predicted non-dimensional drag coefficients for selected test conditions for SCPB test section

Test #	Re_m	KTA		Ergun		Eisfeld and Schnitzlein	
		Ψ (Analytical)	Ψ (SAM results)	Ψ (Analytical)	Ψ (SAM results)	Ψ (Analytical)	Ψ (SAM results)
1	1657.55	3.0520E+00	3.0520E+00	3.6810E+00	3.6811E+00	2.8805E+00	2.8806E+00
2	3315.10	2.7640E+00	2.7640E+00	3.5905E+00	3.5905E+00	2.7843E+00	2.7842E+00
3	4972.65	2.6258E+00	2.6259E+00	3.5603E+00	3.5603E+00	2.7522E+00	2.7522E+00
4	6630.20	2.5371E+00	2.5371E+00	3.5452E+00	3.5451E+00	2.7361E+00	2.7358E+00
5	8287.75	2.4725E+00	2.4727E+00	3.5362E+00	3.5361E+00	2.7265E+00	2.7263E+00

Table C-4 SAM-predicted non-dimensional drag coefficients for selected test conditions for SAPB test section

Test #	Re_m	KTA		Ergun		Eisfeld and Schnitzlein	
		Ψ (Analytical)	Ψ (SAM results)	Ψ (Analytical)	Ψ (SAM results)	Ψ (Analytical)	Ψ (SAM results)
1	1651.80	3.0537E+00	3.0537E+00	3.6816E+00	3.6815E+00	2.9380E+00	2.9378E+00
2	3303.60	2.7653E+00	2.7653E+00	3.5908E+00	3.5909E+00	2.8373E+00	2.8373E+00
3	4955.40	2.6270E+00	2.6269E+00	3.5605E+00	3.5605E+00	2.8037E+00	2.8038E+00
4	6607.20	2.5381E+00	2.5383E+00	3.5454E+00	3.5452E+00	2.7869E+00	2.7867E+00
5	8259.00	2.4735E+00	2.4736E+00	3.5363E+00	3.5363E+00	2.7769E+00	2.7767E+00

Nuclear Science and Engineering Division
Argonne National Laboratory
9700 South Cass Avenue, Bldg. 208
Argonne, IL 60439

www.anl.gov